IEEE Transactions on Industrial Electronics Vol. 59, No. 1, pp. 58-70, January 2012.

A Review of Control and Modulation Methods for Matrix Converters

J. Rodriguez
M. Rivera
J. W. Kolar
P. W. Wheeler

A Review of Control and Modulation Methods for Matrix Converters

Jose Rodriguez, *Fellow, IEEE*, Marco Rivera, *Member, IEEE*, Johan W. Kolar, *Fellow, IEEE*, and Patrick W. Wheeler, *Member, IEEE*

***Abstract*—This paper presents a review of the most popular control and modulation strategies studied for matrix converters (MCs) in the last decade. The purpose of most of these methods is to generate sinusoidal current on the input and output sides. These methods are compared considering theoretical complexity and performance. This paper concludes that the control strategy has a significant impact on the resonance of the MC input filter.**

***Index Terms*—AC–AC conversion, control strategies, matrix converter (MC), modulation schemes.**

I. Introduction

A MATRIX CONVERTER (MC) consists of an array of bidirectional switches, which are used to directly connect the power supply to the load without using any dc-link or large energy storage elements [1].

The most important characteristics of MCs are as follows [2], [3]: 1) a simple and compact power circuit; 2) generation of load voltage with arbitrary amplitude and frequency; 3) sinusoidal input and output currents; 4) operation with unity power factor; and 5) regeneration capability. These highly attractive characteristics are the reason for the tremendous interest in this topology.

The intensive research on MCs starts with the work of Venturini and Alesina in 1980 [2]. They provided the rigorous mathematical background and introduced the name "matrix converter," elegantly describing how the low-frequency behaviors of the voltages and currents are generated at the load and the input. One of the biggest difficulties in the operation of this converter was the commutation of the bidirectional switches [4]. This problem has been solved by introducing intelligent and soft commutation techniques, giving new momentum to research in this area.

Manuscript received November 15, 2010; revised January 31, 2011, April 3, 2011, June 12, 2011, and August 12, 2011; accepted August 12, 2011. Date of publication August 18, 2011; date of current version October 4, 2011. This work was supported in part by the Centro Científico–Tecnológico de Valparaíso under Grant FB0821 and in part by Universidad Técnica Federico Santa María.

J. Rodriguez and M. Rivera are with the Department of Electronics Engineering, Universidad Técnica Federico Santa María, Valparaíso 2390123, Chile (e-mail: jrp@usm.cl; marco.rivera@usm.cl).

J. W. Kolar are with the Power Electronic Systems Laboratory, Swiss Federal Institute of Technology (ETH) Zurich, 8092 Zurich, Switzerland (e-mail: kolar@lem.ee.ethz.ch).

P. W. Wheeler is with the School of Electrical and Electronic Engineering, The University of Nottingham, NG7 2RD Nottingham, U.K. (e-mail: Pat.Wheeler@nottingham.ac.uk).

Color versions of one or more of the figures in this paper are available online at http://ieeexplore.ieee.org.

Digital Object Identifier 10.1109/TIE.2011.2165310

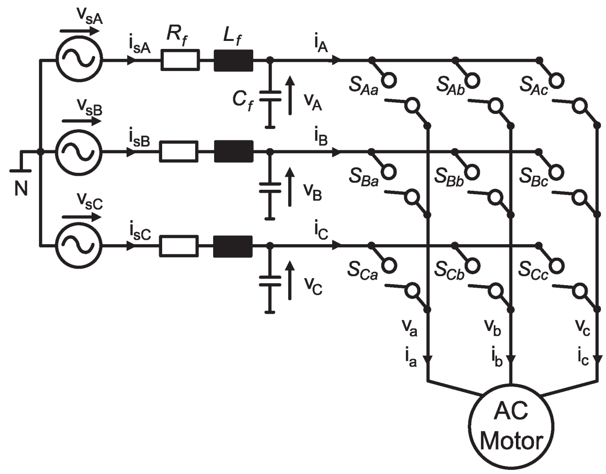

Fig. 1. DMC topology.

After almost three decades of intensive research, the development of this converter is reaching industrial application. In effect, at least one big manufacturer of power converters (Yaskawa) is now offering a complete line of standard units for up to several megawatts and medium voltage using cascade connection. These units have rated power (voltages) of 9–114 kVA (200 and 400 V) for low-voltage MC and 200–6.000 kVA (3.3 and 6.6 kV) for medium voltage [1]. Years of continuous effort have been dedicated to the development of different modulation and control strategies that can be applied to MCs [4]–[11].

This paper presents the most relevant control strategies for MCs and gives an assessment of them in terms of performance and complexity.

II. Power Circuit and Working Principle of the DMC

A direct MC (DMC) is a single-stage converter with $m \times n$ bidirectional power switches that connects an m-phase voltage source to an n-phase load [2], [12]. The DMC of 3 × 3 switches, shown in Fig. 1, is the most important from a practical point of view because it connects a three-phase source to a three-phase load, typically a motor

$$S_{ij}(t) = \begin{cases} 1, & \text{switch on} \\ 0, & \text{switch off.} \end{cases} \quad (1)$$

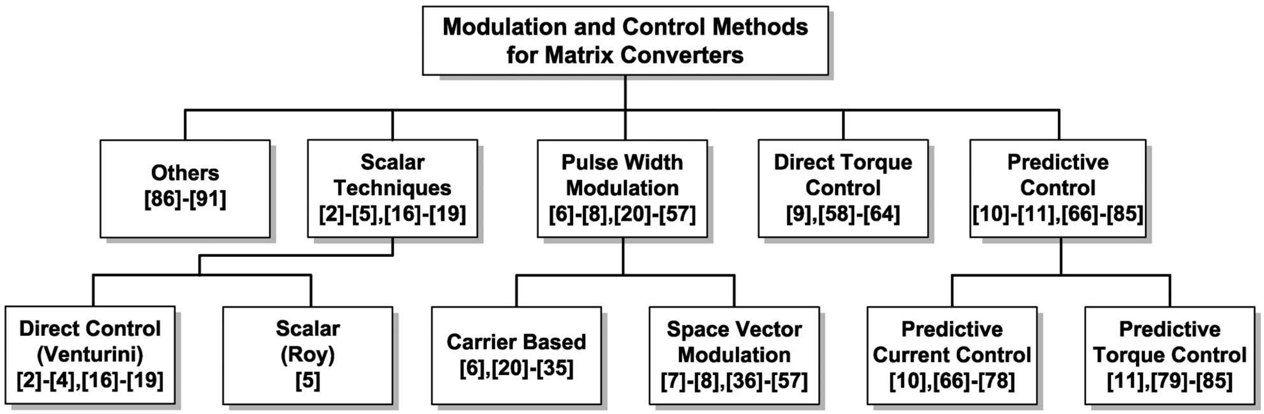

Fig. 2. Summary of modulation and control methods for MCs.

The power filter (R_f, L_f, C_f) located at the input of the converter mitigates the high-frequency components of the MC input currents, generating almost sinusoidal source currents and avoiding the generation of overvoltages. Overvoltages are caused by the fast commutation of input currents due to the presence of the short-circuit reactance of any real power supply. The inductance of the input filter L_f and capacitor C_f provide series resonance for any harmonic coming from the three-phase mains and parallel resonance for current harmonics generated in currents i_A, i_B, and i_C through the operation of the switches. When the frequency of these harmonics is close to the resonance frequency of the filter, strong oscillations will appear. The design of the input filter is an important issue in the operation of the DMC. Design guidelines for the filter can be found in [13]–[15].

The switching function of a single switch is defined as follows.

Due to the presence of capacitors at the input of the DMC, only one switch on each column can be closed. Furthermore, the inductive nature of the load makes it impossible to interrupt the load current suddenly, and therefore, at least one switch of each column must be closed.

In order to develop a modulation strategy for the MC, it is necessary to develop a mathematical model, which can be derived directly from Fig. 1, as follows:

$$\mathbf{v_o} = \mathbf{T}(S_{ij})\mathbf{v_i} \tag{2}$$

$$\mathbf{i_i} = \mathbf{T}(S_{ij})^{\mathrm{T}}\mathbf{i_o} \tag{3}$$

where $\mathbf{v_o} = [v_a \ v_b \ v_c]^{\mathrm{T}}$ is the output voltage vector, $\mathbf{v_i} = [v_A \ v_B \ v_C]^{\mathrm{T}}$ is the input voltage vector, $\mathbf{i_i} = [i_A \ i_B \ i_C]^{\mathrm{T}}$ is the input current vector, $\mathbf{i_o} = [i_a \ i_b \ i_c]^{\mathrm{T}}$ is the output current vector, and $\mathbf{T}(S_{ij})$ is the instantaneous transfer matrix of the DMC as a function of the switches S_{ij} [12], which is defined as

$$\mathbf{T}(S_{ij}) = \begin{bmatrix} S_{Aa} & S_{Ba} & S_{Ca} \\ S_{Ab} & S_{Bb} & S_{Cb} \\ S_{Ac} & S_{Bc} & S_{Cc} \end{bmatrix}. \tag{4}$$

Equations (2) and (3) are the basis of all modulation methods, which consist of selecting appropriate combinations of open and closed switches to generate the desired output voltages.

III. General Classification of Control and Modulation Methods

The most relevant control and modulation methods developed up to now, for the MC, are shown in Fig. 2. The first and highly relevant method is called the direct transfer function approach also known as the Venturini method. Here, the output voltage is obtained by the product of the input voltage and the transfer matrix representing the converter. Another strategy is the scalar method developed by Roy, which consists of using the instantaneous voltage ratio of specific input phase voltages to generate the active and zero states of the converter's switches. A very important solution for the control of MCs comes from the use of pulsewidth modulation (PWM) techniques previously developed for voltage source inverters. The simplest approach is to use carrier-based PWM techniques. A very elegant and powerful solution currently in use is to apply space-vector modulation (SVM) in MCs. An alternative solution is direct torque and flux control, which has also been proposed for the speed control of an ac machine driven by this converter. More modern techniques, such as predictive control, have recently been proposed for the current and torque control of ac machines using MCs. In the following pages, a description and a comparison of these technologies will be presented.

IV. Scalar Techniques

A. *Direct Method: Venturini*

Modulation is the procedure used to generate the appropriate firing pulses to each of the nine bidirectional switches (S_{ij}). This method was proposed by Venturini in [2] and has been used since, as reported in [3], [4], [12], and [16]–[19]. In this case, the objective of the modulation is to generate variable frequency and variable amplitude sinusoidal output voltages (v_{jN}) from the fixed-frequency and fixed-amplitude input voltages (V_i). Here, the instantaneous input voltages are used to synthesize a signal whose low-frequency component is the desired output voltage.

If t_{ij} is defined as the time during which switch S_{ij} is on and T_s as the sampling interval, we can express the aforementioned synthesis principle as

$$\overline{v}_{jN} = \frac{t_{Aj}v_A + t_{Bj}v_B + t_{Cj}v_C}{T_s} \tag{5}$$

where $\overline{v}_{jN}$ is the low-frequency component (mean value calculated over one sampling interval) of the jth output phase and changes in each sampling interval. With this strategy, a high-frequency switched output voltage is generated, but a fundamental component has the desired waveform.

Obviously, $T_s = t_{Aj} + t_{Bj} + t_{Cj}\ \forall j$, with $j = a, b, c$, and therefore, the following duty cycles can be defined:

$$m_{Aj}(t) = \frac{t_{Aj}}{T_s} \qquad m_{Bj}(t) = \frac{t_{Bj}}{T_s} \qquad m_{Bj}(t) = \frac{t_{Bj}}{T_s}. \tag{6}$$

Extending (5) to each output phase and using (6), the following equation can be derived:

$$\overline{\mathbf{v}}_{\mathbf{o}}(t) = \mathbf{M}(t)\mathbf{v}_{\mathbf{i}}(t) \tag{7}$$

where $\overline{\mathbf{v}}_{\mathbf{o}}(t)$ is the low-frequency output voltage vector, $\mathbf{v}_{\mathbf{i}}(t)$ is the instantaneous input voltage vector, and $\mathbf{M}(t)$ is the low-frequency transfer matrix of the converter, defined as

$$\mathbf{M}(t) = \begin{bmatrix} m_{Aa}(t) & m_{Ba}(t) & m_{Ca}(t) \\ m_{Ab}(t) & m_{Bb}(t) & m_{Cb}(t) \\ m_{Ac}(t) & m_{Bc}(t) & m_{Cc}(t) \end{bmatrix}. \tag{8}$$

Following an analogous procedure for the input current, it can be easily shown that:

$$\bar{\mathbf{i}}_{\mathbf{i}}(t) = \mathbf{M}^{\mathrm{T}}(t)\mathbf{i}_{\mathbf{o}}(t) \tag{9}$$

where $\bar{\mathbf{i}}_{\mathbf{i}}(t)$ is the low-frequency-component input current vector, $\mathbf{i}_{\mathbf{o}}(t)$ is the instantaneous output current vector, and $\mathbf{M}^{\mathrm{T}}(t)$ is the transpose of $\mathbf{M}(t)$. Equations (7) and (9) are the basis of the Venturini modulation method, leading to the conclusion that the low-frequency components of the output voltages are synthesized with the instantaneous values of the input voltages and that the low-frequency components of the input currents are synthesized with the instantaneous values of the output currents. Suppose that the input voltages $\mathbf{v}_{\mathbf{i}}$ are given by

$$\mathbf{v}_{\mathbf{i}}(t) = \begin{bmatrix} V_i \cos(w_i t) \\ V_i \cos(w_i t - 2\pi/3) \\ V_i \cos(w_i t + 2\pi/3) \end{bmatrix} \tag{10}$$

and that, due to the low-pass characteristic of the load, the output currents $\mathbf{i}_{\mathbf{o}}$ are sinusoidal and can be expressed as

$$\mathbf{i}_{\mathbf{o}}(t) = \begin{bmatrix} I_o \cos(w_o t + \phi_o) \\ I_o \cos(w_o t - 2\pi/3 + \phi_o) \\ I_o \cos(w_o t + 2\pi/3 + \phi_o) \end{bmatrix} \tag{11}$$

with $w_i = 2\pi f_i$ and $w_o = 2\pi f_o$, where f_i and f_o correspond to the source and load frequencies, respectively. V_i corresponds to the input voltage amplitude, and I_o corresponds to the output current amplitude. Furthermore, suppose that the desired input current vector $\mathbf{i}_{\mathbf{i}}$ is given by

$$\mathbf{i}_{\mathbf{i}}(t) = \begin{bmatrix} I_i \cos(w_i t + \phi_i) \\ I_i \cos(w_i t + \phi_i - 2\pi/3) \\ I_i \cos(w_i t + \phi_i + 2\pi/3) \end{bmatrix} \tag{12}$$

with I_i as the input current amplitude. Also, suppose that the desired output voltage $\mathbf{v}_{\mathbf{o}}$ can be expressed as follows:

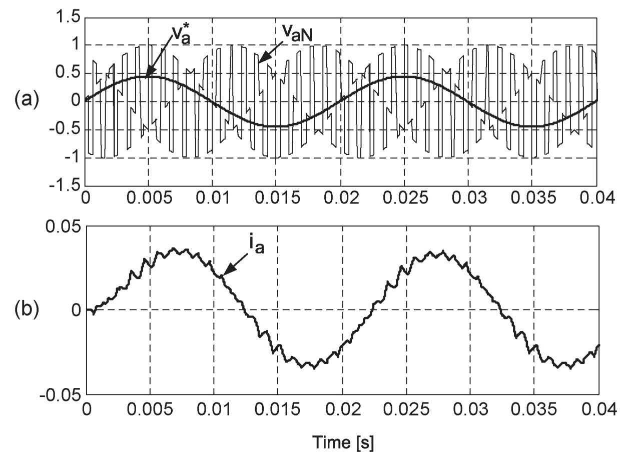

Fig. 3. Direct method: Venturini, typical waveforms. (a) Output voltage v_{aN} [in per unit (p.u.)], (bold line) its reference and (b) output current i_a (in p.u.).

$$\mathbf{v}_{\mathbf{o}}(t) = \begin{bmatrix} qV_i \cos(w_o t) \\ qV_i \cos(w_o t - 2\pi/3) \\ qV_i \cos(w_o t + 2\pi/3) \end{bmatrix} \tag{13}$$

and that the following active power balance equation must be satisfied

$$P_o = \frac{3qV_i I_o \cos(\phi_o)}{2} = \frac{3V_i I_i \cos(\phi_i)}{2} = P_i \tag{14}$$

where P_o and P_i are the output and input active powers, respectively, ϕ_i is the input displacement angle, and q is the voltage gain of the MC. With the previous definitions, the modulation problem is reduced to finding a low-frequency transfer matrix $\mathbf{M}(t)$ such that (7) and (9) are satisfied. The explicit form of the matrix $\mathbf{M}(t)$ can be obtained from [2] and [12], and it can be reduced to the following expression:

$$m_{ij}(t) = \frac{1}{3}\left(1 + 2v_{iN}(t)\overline{v}_{jN}/V_i^2\right) \tag{15}$$

where $i = A, B, C$ and $j = a, b, c$.

An important aspect of the solution presented is that the voltage gain of the converter cannot exceed $q = 0.5$ due to the working principle (mean value) and the input voltage waveforms. To increase the gain voltage to $q = \sqrt{3}/2 = 0.866$, Venturini proposed the injection of a third harmonic, resulting in the following expression:

$$m_{ij}(t) = \frac{1}{3}\left(1 + \frac{2v_{iN}(t)\overline{v}_{jN}}{V_i^2} + \frac{4q}{3\sqrt{3}}\zeta\right) \tag{16}$$

with $\zeta = \sin(w_i t + \beta_i)\sin(3w_i t)$ for $i = A, B, C$, $j = a, b, c$, and $\beta_i = 0, (2\pi/3), (4\pi/3)$. The same gain voltage $q = \sqrt{3}/2$ can be obtained by using the line-to-line voltages in the modulation. Typical waveforms of the output voltage and current are shown in Fig. 3.

B. Roy's Method

The scalar method, which was proposed in 1987 by Roy and April in [5], consists of using the instantaneous voltage ratio of specific input phase voltages to generate the active and zero states of the converter's switches. The value of any instantaneous output phase voltage $(j = a, b, c)$ is expressed as follows:

$$v_{jN} = \frac{1}{T_s}(t_K v_K + t_L v_L + t_M v_M) \tag{17}$$

$$t_K + t_L + t_M = T_s \tag{18}$$

according to two rules, where the subscript M is assigned to the input voltage which has a different polarity to the other two inputs. The subscript L is assigned to the smallest of the other two input voltage magnitudes, and subscript K is assigned to the third input voltage. Equations (17) and (18) are similar to the ones proposed by Venturini, as mentioned in the previous section. In this case, the switching patterns depend only on the scalar comparison of input phase voltages and the instantaneous value of the desired output voltage. So, the duty cycles are given as indicated in

$$\left.\begin{array}{l} m_{Lj} = \frac{(v_{jN}-v_M)v_L}{1.5V_i^2} \\ m_{Kj} = \frac{(v_{jN}-v_M)v_K}{1.5V_i^2} \\ m_{Mj} = 1-(m_{Lj}+m_{Kj}) \end{array}\right\} \tag{19}$$

for $j = a, b, c$, respectively. As with the previously presented basic solution for the modulation problem, the voltage transfer ratio is limited to $q \leq 0.5$, in order to yield positive values for times t_K, t_L, and t_M. By modifying the switching time of the basic scalar control law, it is possible to add the third harmonic to obtain an overall voltage transfer ratio of $q = \sqrt{3}/2$. So, the modulation duty cycles for the scalar method can be represented by [5]

$$m_{ij} = \frac{1}{3}\left(1 + \frac{2v_i v_j}{V_i^2} + \frac{2}{3}\zeta\right) \tag{20}$$

for $i = A, B, C$, $j = a, b, c$, and $\beta_k = 0, (2\pi/3), (4\pi/3)$.

Equations (16) and (20) are equal when the output voltage is maximum $(q = \sqrt{3}/2)$. The difference between the methods is that the term q is used in the Venturini method and is fixed at its maximum value in the scalar method. The effect on the output voltage is negligible, except at low switching frequencies, where the Venturini method is superior.

C. Current Phase Displacement Control for Venturini and Roy Methods

According to [5] and [12], by intentionally shifting or delaying the timing sequence with respect to the zero crossing of the associated input phase voltage, it is possible to shift current $\mathbf{i_i}$ relative to $\mathbf{v_i}$ $(i = A, B, C)$, therefore altering the input power displacement factor.

Let us define the following fictitious phase voltages at the input part of the MC as

$$\left.\begin{array}{l} v'_A = V_i \sin(w_i t + \Delta\phi) \\ v'_B = V_i \sin\left(w_i t + \Delta\phi - \frac{2\pi}{3}\right) \\ v'_C = V_i \sin\left(w_i t + \Delta\phi + \frac{2\pi}{3}\right) \end{array}\right\} \tag{21}$$

where $\Delta\phi$ is the displacement factor angle between the measured input voltage vector $\mathbf{v_i}$ and the input current vector $\mathbf{i_i}$.

For Venturini's method, the solution of the new m'_{ij} is given by

$$m'_{ij}(t) = \frac{1}{3}\left(1 + \frac{2v'_{iN}(t)\overline{v}_{jN}}{V_i^2} + \frac{4q}{3\sqrt{3}}\zeta\right) \tag{22}$$

for $i = A, B, C$.

For Roy's method, let us now assign M, K, and L to A', B', and C' according to the rules mentioned before. Then

$$\left.\begin{array}{l} m'_{Lj} = \frac{(v_{jN}-v'_M)v'_L}{1.5V_i^2} \\ m'_{Kj} = \frac{(v_{jN}-v'_M)v'_K}{1.5V_i^2} \\ m'_{Mj} = 1-\left(m'_{Lj}+m'_{Kj}\right) \end{array}\right\} \tag{23}$$

for $j = a, b, c$, respectively. Of course, the desired output voltage v_{jN} is still expressed by (13) or (17), for Venturini or Roy methods, respectively.

It follows that the input currents $\mathbf{i_i}$ will be in phase with their respective fictitious voltages. However, they will be displaced by an angle $\Delta\phi$ according to the real voltage $\mathbf{v_i}$. So, the input power displacement factor is totally controllable by proper adjustment of the timing sequence, regardless of the load characteristic.

In both methods, a reduction of the voltage transfer ratio is observed as the power displacement factor is reduced, as indicated in [5].

V. PWM Methods

A. Carrier-Based Modulation Method

Many control strategies based on PWM methods which allow for output voltage regulation while maintaining unity power factor on the input side have been applied to different kinds of MCs, as has been reported in [6] and [20]–[35]. For simplicity, we will discuss a carrier-based modulation method applied to a three-phase-to-single-phase MC, which can be easily extended to a three-phase-to-three-phase or multilevel converter. The technique is based on a sinusoidal PWM (SPWM), which is a well-known shaping technique in power electronics where a high-frequency triangular carrier signal v_{tri} is compared with a sinusoidal reference signal $\mathbf{v_o}$, as shown in Fig. 4 [6], [22]. In this method, the switching pulses are generated by using a logical table as a function of the input voltages and the desired levels on the output side. The different input voltage states are identified by considering variables x_A, x_B, and x_C, which are generated according Table I. If the conditions given in Table I are not satisfied, the logic variable take the value 0. The gate pulse pattern generation of the MC is given according to a switching state selector generated by the following equation:

$$N = 16x_A + 8x_B + 4x_C + 2L_1 + L_0 \tag{24}$$

where L_0 and L_1 are the output voltage levels (L_0 is selected if the level of the output voltage reference is less than or equal to zero, and L_1 is selected if the output voltage level is above zero). Generally, PWM methods can work with a variable input power factor, as demonstrated in [35], where it is possible to synthesize the sinusoidal input currents with a desired power

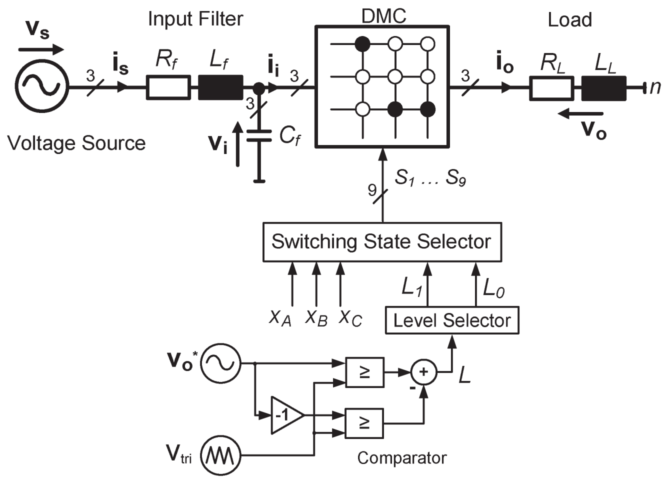

Fig. 4. Unipolar SPWM method and desired output level voltage.

TABLE I
PWM METHOD: INPUT VOLTAGE STATES

Condition	Value
$v_A > v_B$	$x_A = 1$
$v_B > v_C$	$x_B = 1$
$v_C > v_A$	$x_C = 1$

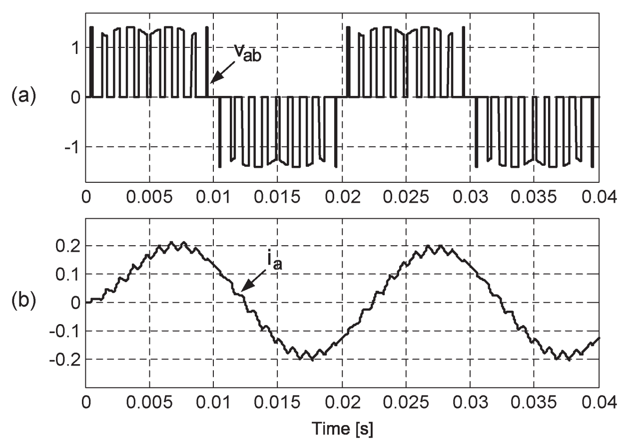

Fig. 5. Carrier-based method, typical waveforms. (a) Line-to-line output voltage v_{ab} (in p.u.) and (b) output current i_a (in p.u.).

factor by changing the slope of the carrier and using the offset voltages. However, the PWM method presented in this paper is restricted in its operation with unity power factor, due to its simplicity. Typical waveforms of output voltage and current are shown in Fig. 5. More details about this method can be found in [6] and [22].

B. SVM Method

This method has been proposed in [7], [8], [36], and [37]. The space-vector approach is based on the instantaneous space-vector representation of input and output voltages and currents. Among the 27 possible switching configurations available in three-phase MCs, only 21 are useful in the SVM algorithm. The first 18 switching configurations determine an output voltage vector and an input current vector, having fixed directions (Fig. 6). The magnitude of these vectors depends upon the instantaneous values of the input voltages and output line

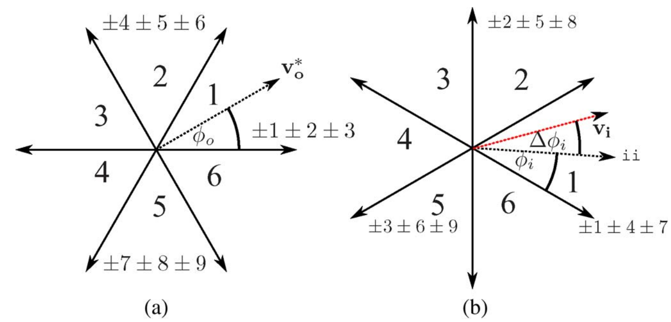

Fig. 6. Available DMC vectors for SVM. (a) Voltage vectors. (b) Current vectors.

currents, respectively. The last three switching configurations determine zero input current and output voltage vectors. The SVM algorithm for MCs has the inherent capability to achieve full control of both the output voltage vector and the instantaneous input current displacement angle [7], [8], [36]–[57]. The two-stage SVM method [54] is a variation of the classic SVM technique which has some important features such as overmodulation, but this method is no longer used.

At any given sampling instant, the output voltage vector and the input current displacement angle are known as reference quantities. The input line-to-neutral voltage vector is imposed by the source voltages and is recognized by its measurements. Then, the control of the input side can be achieved, controlling the phase angle of the input current vector. Both input current and output voltage vectors are synthesized by considering the duty cycles. The duty cycles are calculated based on the phase of output voltage and input current vector references such as in the following (Fig. 6) [37]:

$$\delta_1 = -1^{K_v+K_i+1}\frac{2m}{\sqrt{3}}\frac{\cos\left(\phi_o'-\frac{\pi}{2}\right)\cos\left(\phi_i'-\frac{\pi}{2}\right)}{\cos(\Delta\phi)} \tag{25}$$

$$\delta_2 = -1^{K_v+K_i}\frac{2m}{\sqrt{3}}\frac{\cos\left(\phi_o'-\frac{\pi}{2}\right)\cos\left(\phi_i'+\frac{\pi}{6}\right)}{\cos(\Delta\phi)} \tag{26}$$

$$\delta_3 = -1^{K_v+K_i}\frac{2m}{\sqrt{3}}\frac{\cos\left(\phi_o'+\frac{\pi}{6}\right)\cos\left(\phi_i'-\frac{\pi}{2}\right)}{\cos(\Delta\phi)} \tag{27}$$

$$\delta_4 = -1^{K_v+K_i+1}\frac{2m}{\sqrt{3}}\frac{\cos\left(\phi_o'+\frac{\pi}{6}\right)\cos\left(\phi_i'+\frac{\pi}{6}\right)}{\cos(\Delta\phi)} \tag{28}$$

where m is the modulation index; $\Delta\phi$ is the displacement angle between the measured input voltage vector $\mathbf{v_i}$ and the input current reference vector $\mathbf{i_i^*}$; K_v and K_i are the voltage and current sectors, respectively; and

$$\phi_o' = \phi_o - (K_v-1)\frac{\pi}{6} \qquad \phi_i' = \phi_i - (K_i-1)\frac{\pi}{6}. \tag{29}$$

If the sign of any duty cycle is negative, then the name of the switching state to apply must have a negative sign. The duty cycle δ_0 of the zero vector is such that the total duty cycle must be equivalent to the unit at a fixed sampling frequency, i.e.,

$$\delta_0 = 1-\delta_1-\delta_2-\delta_3-\delta_4. \tag{30}$$

Assuming a displacement power factor of one on the input side of the DMC, i.e., $\Delta\phi = 0$, the maximum modulation index is $m = \sqrt{3}/2$.

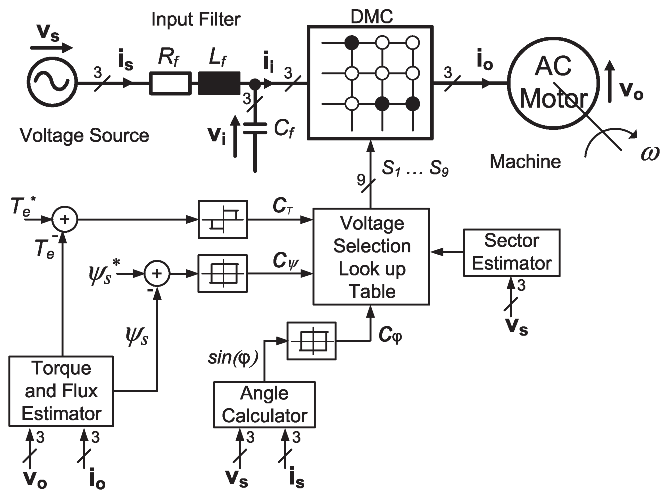

Fig. 7. DTC scheme.

VI. DTC

Today, direct torque control (DTC) is established as a high-performance torque and flux control method for ac machines fed by voltage source inverters [9], [58].

This method is based on the torque equation of the machine which is expressed as a function of the angle between the stator and rotor flux vectors in the following way:

$$T_e = k_T(\psi_{r\alpha}\psi_{s\beta} - \psi_{r\beta}\psi_{s\alpha}) \tag{31}$$

with $k_T = (3/2)p(L_m/L_rL_s - L_m^2)$, (where L_r, L_s, and L_m are the self-inductance and mutual inductance, respectively). The method is also based on the fact that changes in the voltage delivered by the inverter directly affect the behavior of the machine's stator flux, as shown by

$$\boldsymbol{\psi}_\mathbf{s}(k+1) = \boldsymbol{\psi}_\mathbf{s}(k) + T_s\mathbf{v_s}(k+1) - R_sT_s\mathbf{i_s}(k). \tag{32}$$

In [59], the authors proposed that DTC controls an ac machine by using an MC. As shown in Fig. 7, this method uses a nonlinear hysteresis comparator to control the torque, which delivers the control variable c_T. An additional hysteresis controller is used to create another closed loop to control the flux, which delivers the variable c_ψ. A third loop is used to control the power factor of the input current by controlling the displacement factor $\Delta\phi$ with another nonlinear controller, which delivers variable c_φ. These variables c_T, c_ψ, and c_φ, in conjunction with the position of the stator flux, reveal which direction to select the gate drive pulses in the lookup table for the bidirectional switches of the MC.

Although lookup tables for DTC using a voltage source inverter are well known and published in several papers and textbooks, the application of this method in an MC has additional complexity. In effect, the selection of a single switching state for the MC is not based exclusively on the information of torque error and flux error. Rather, the designer must know *a priori* what additional effect this switching state will have on the behavior of the input power factor. To obtain this information is complex [60].

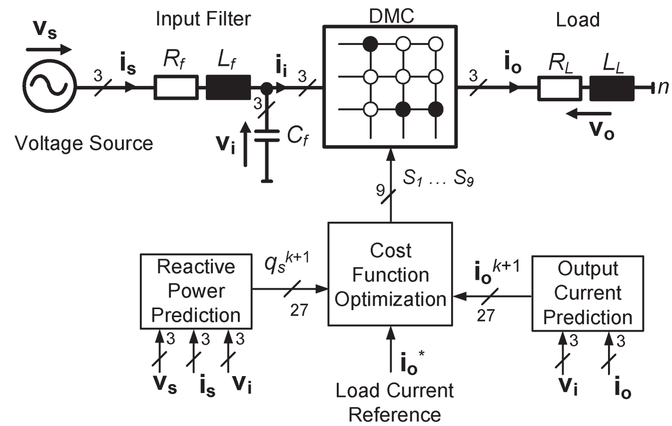

Fig. 8. PCC scheme.

The results of this method generally show very good performance dynamics in the control of the machine. However, the input filter of the MC presents higher resonances. To improve the general drive performance, the use of DTC in MCs is a subject of intensive study today. Some works are focused on improving the behavior of the input filter [60]–[64].

VII. Predictive Control

A. PCC

Owing to advances in processors, predictive control schemes have recently emerged as feasible approaches [65]. A predictive current control (PCC) scheme is shown in Fig. 8. It shows the converter's switching state selection that leads the controlled variables closest to their respective references at the end of the sampling period. This strategy uses the converter and load models to predict the future behavior of load currents and reactive power. A simple but functional time-continuous model of the load side can be expressed as

$$\frac{d\mathbf{i_o}}{dt} = \frac{1}{L_L}\mathbf{v_o} - \frac{R_L}{L_L}\mathbf{i_o}. \tag{33}$$

The state variable model of the ac-input side is given from Fig. 1 as follows:

$$\frac{d\mathbf{i_s}}{dt} = \frac{1}{L_f}(\mathbf{v_s} - \mathbf{v_i} - R_f\mathbf{i_s}) \tag{34}$$

$$\frac{d\mathbf{v_i}}{dt} = \frac{1}{C_f}(\mathbf{i_s} - \mathbf{i_i}). \tag{35}$$

Given the first-order nature of the load model, a first-order discrete approximation allows the future load current to be predicted as

$$\mathbf{i_o}(k+1) = \frac{T_s\mathbf{v_o}(k+1) + L_L\mathbf{i_o}(k)}{L_L + R_LT_s} \tag{36}$$

where T_s corresponds to the sampling time. On the input side, the equations represent a second-order model. As such, an exact discrete state model is best used to obtain the supply current in the sampling instant $k+1$, in order to predict the future reactive power. So, the general expression to predict the line input current is

$$\mathbf{i_s}(k+1) = c_1\mathbf{v_s}(k) + c_2\mathbf{v_i}(k) + c_3\mathbf{i_s}(k) + c_4\mathbf{i_i}(k) \tag{37}$$

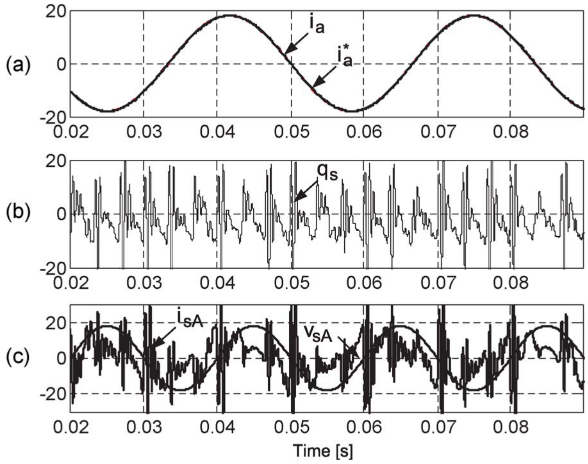

Fig. 9. PCC without power factor correction $A = 0$. (a) Output current (in amperes). (b) Reactive power (in kvar). (c) Input current (in amperes) and input voltage (V/30).

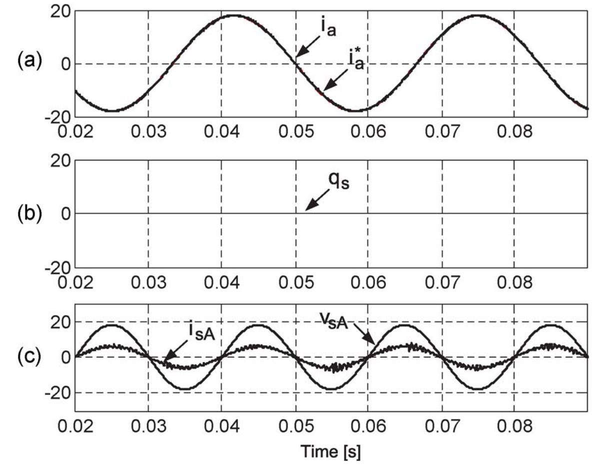

Fig. 10. PCC with power factor correction $A = 1$. (a) Output current (in amperes). (b) Reactive power (in kvar). (c) Input current (in amperes) and input voltage (V/30).

where c_i $(i = 1, 2, 3, 4)$ values are calculated such that the discrete model provides the exact values of the continuous system. Two main conditions must be fulfilled for the converter to operate properly: First, the line side of the converter must minimize the instantaneous reactive power, and second, the load current must follow the reference with good accuracy. Both requirements can be merged into a single quality function g as follows:

$$g = \triangle i_o(k + 1) + A\triangle q_s(k + 1) \tag{38}$$

where

$$\triangle i_o(k+1) = |i^*_{o\alpha} - i_{o\alpha}(k+1)| + |i^*_{o\beta} - i_{o\beta}(k+1)| \tag{39}$$

$$\triangle q_s(k+1) = |v_{s\alpha}(k+1) i_{s\beta}(k+1) - v_{s\beta}(k+1) i_{s\alpha}(k+1)|. \tag{40}$$

The first term considers the comparison between the reference load currents and the predicted ones. The second term corresponds to the predicted input reactive power. Both are expressed in α–β components.

The control method operates as follows: At each sampling time, all 27 possible switching states are used to calculate the predicted values of the load and input current, allowing the evaluation of function g in (38). After that, the valid switching state that produces the minimum value of g is selected for the next modulation period. Fig. 9 shows the behavior of the DMC when the quality function has a value of $A = 0$, for the weighting factor. The load current i_a is sinusoidal, and the reactive power has high values. In this case, the input current presents very high distortion, which is originated by a strong resonance of the input filter. Fig. 10 shows the behavior of the DMC when a control of the input power factor is being considered. This is achieved by increasing the value of the weighting factor $A = 1$. It can be observed that the load current i_a is sinusoidal and that the input reactive power is zero. This new control strategy practically eliminates the resonance of the input filter. The improvement in the quality of the input current is remarkable.

Different techniques for MCs have been proposed under the name of PCC, as reported in [10] and [66]–[78]. In [67], a PCC for an induction machine (IM) fed by an MC is developed by considering a classic stage that handles speed, flux, and torque control. It does this by means of field-oriented control, which generates the reference currents for the predictive stage. A similar idea is presented in [70] to control a permanent-magnet synchronous machine. Using this scheme, it is also feasible to control other variables within an electrical system, for example, minimizing common-mode voltage, reported in [68], or increasing efficiency and reducing switching losses, as presented in [69]. Recently, this idea has been extended to indirect MCs, as reported in [73], [74], and [76].

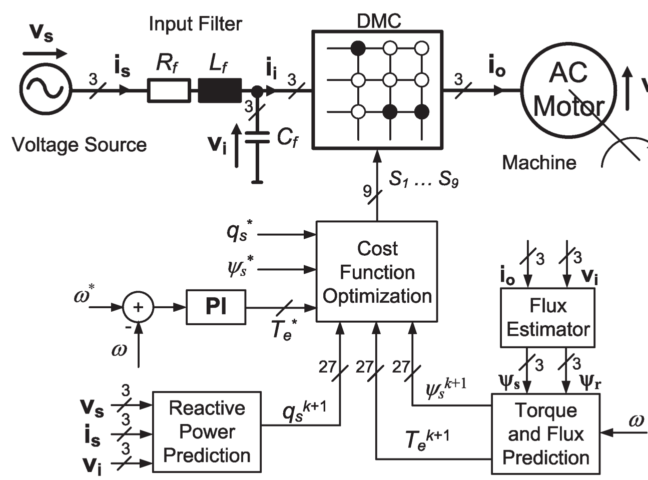

Fig. 11. PTC scheme.

B. PTC

A diagram of the predictive torque control (PTC) strategy is shown in Fig. 11. This control method has been introduced in [11] and [79]–[85]. Similar to the previously explained method, PTC consists of choosing, at fixed sampling intervals, one of the 27 feasible switching states of the DMC. The selection of the switching state for the following time interval is performed using a quality function minimization technique. This quality function g represents the evaluation criteria in order to select the best switching state for the next sampling interval. For the computation of g, the input current vector $\mathbf{i_s}$, the electric torque T_e, and the stator flux $\boldsymbol{\psi}_\mathbf{s}$ in the next sampling interval are predicted, assuming the application of each valid switching state, by means of a mathematical model of the input filter and the IM. A PI controller is used to generate the reference torque T_e^* to the predictive algorithm. A mathematical discrete-time model is derived to predict the behavior of the system under a given switching state, based on the well-known dynamic equations for an IM [11], [79]–[81]. The stator and rotor voltage equations in fixed stator coordinates for a squirrel-cage IM can be presented as

$$\mathbf{v_o} = R_s \mathbf{i_o} + \frac{d\boldsymbol{\psi}_\mathbf{s}}{dt} \tag{41}$$

$$\mathbf{v_r} = R_r \mathbf{i_r} + \frac{d\boldsymbol{\psi}_\mathbf{r}}{dt} - jp\omega\psi_r = 0 \tag{42}$$

where R_s and R_r are the stator and rotor resistances, $\boldsymbol{\psi}_\mathbf{s}$ and $\boldsymbol{\psi}_\mathbf{r}$ are the stator and rotor fluxes, ω is the mechanical rotor speed, and p is the number of pole pairs of the IM.

The stator and rotor fluxes are related to the stator and rotor currents by

$$\boldsymbol{\psi}_\mathbf{s} = L_s \mathbf{i_o} + L_m \mathbf{i_r} \tag{43}$$

$$\boldsymbol{\psi}_\mathbf{r} = L_m \mathbf{i_o} + L_r \mathbf{i_r} \tag{44}$$

where L_s, L_r, and L_m are the self-inductance and mutual inductance, respectively. Finally, the electric torque produced by the machine can be obtained by

$$T_e = \frac{3}{2} p\xi \mathrm{Im}\{\bar{\boldsymbol{\psi}}_\mathbf{r} \boldsymbol{\psi}_\mathbf{s}\} = \frac{3}{2} p\xi(\psi_{r\alpha}\psi_{s\beta} - \psi_{r\beta}\psi_{s\alpha}) \tag{45}$$

where $\xi = L_m/L_r L_s - L_m^2$, $\bar{\boldsymbol{\psi}}_\mathbf{r}$ is the complex conjugate of vector $\boldsymbol{\psi}_\mathbf{r}$, and the subscripts α and β represent the real and imaginary components of the associated vector. Equations (41) and (42) can be rewritten, solving the stator and rotor currents in terms of the stator and rotor fluxes from (43) and (44), as

$$\frac{d\boldsymbol{\psi}_\mathbf{s}}{dt} = \frac{-R_s L_r}{L_r L_s - L_m^2}\boldsymbol{\psi}_\mathbf{s} + \frac{R_s L_m}{L_r L_s - L_m^2}\boldsymbol{\psi}_\mathbf{r} + \mathbf{v_o} \tag{46}$$

$$\frac{d\boldsymbol{\psi}_\mathbf{r}}{dt} = \frac{R_r L_m}{L_r L_s - L_m^2}\boldsymbol{\psi}_\mathbf{s} - \frac{R_r L_s}{L_r L_s - L_m^2}\boldsymbol{\psi}_\mathbf{r} - jp\omega\boldsymbol{\psi}_\mathbf{r}. \tag{47}$$

The next step is to define a discrete-time model based on these continuous-time equations. Using a forward Euler approximation [11], the following discrete equations are computed from (46) and (47):

$$\psi_\mathbf{s}(k+1) = (1 - \chi L_r)\boldsymbol{\psi}_\mathbf{s}(k) + \chi L_m \boldsymbol{\psi}_\mathbf{r}(k) + \mathbf{v_o}(k) \tag{48}$$

$$\psi_\mathbf{r}(k+1) = \lambda L_m \boldsymbol{\psi}_\mathbf{s}(k) + (1 - \lambda L_s)\boldsymbol{\psi}_\mathbf{r}(k) - jp\omega(k)\boldsymbol{\psi}_\mathbf{r}(k) \tag{49}$$

where $\chi = T_s R_s / L_r L_s - L_m^2$, $\lambda = T_s R_r / L_r L_s - L_m^2$, and T_s is the sampling period.

If a certain voltage vector $\mathbf{v_o}(k)$ is applied from the DMC, then (45), (48), and (49) are used by the proposed method to predict the stator flux and the electric torque produced by the IM during the next sampling interval. The quality function represents the evaluation criteria to decide which switching state is the best to apply. The function is composed of the absolute error of the predicted torque, the absolute error of the predicted flux magnitude, and the absolute error of the predicted reactive input power, resulting in

$$g = \triangle T_e(k+1) + \lambda_\psi \triangle\psi(k+1) + \lambda_q \triangle q_s(k+1) \tag{50}$$

where λ_Q and λ_ψ are the weighting factors that handle the relation between reactive input power, torque, and flux conditions. This quality function must be calculated for each of the 27 feasible switching states. The state that generates the optimum value (in this case, a minimum) will be chosen and applied during the next sampling period. In that sense, the technique assigns costs to the objectives reflected in g, weighted by λ_T, λ_ψ, and λ_q, and then chooses the switching state that presents the lowest cost. Typical waveforms without and with input factor correction are shown in Figs. 12 and 13, respectively. Both cases present good behavior on the output side. Input currents, on the other hand, present significant differences. Implementing the method with $\lambda_q = 0$, the input current shows high distortion and phase shift with its phase voltage. Using the added term to control the input factor and considering $\lambda_q > 0$, the input current is close to sinusoidal, as shown in Fig. 13.

VIII. Assessment of the Methods

The performance of all methods can be compared considering the following figures of merit:

1) theoretical complexity;
2) quality of load current;
3) dynamic response;
4) sampling frequency;
5) switching frequency,
6) resonance of input filter.

Table II presents a comparison of these methods. In terms of complexity, although carrier-based methods involve many equations, with respect to the other techniques, they are very simple to implement for generating gate drive pulses for bidirectional power switches [29]. Predictive technique [10], [65] is very simple in comparison to SVM [7], [37] and DTC methods, which are complex. In DTC, the engineer must know the effect of any switching state on the behavior of torque, flux, and the input power factor of the MC, which is a complex task [59], [60]. All the methods deliver a high-quality current to the load. The main difference is that some methods work with fixed switching frequency and other strategies, such as DTC and PTC, work with variable switching frequency. It can also be observed that some methods operate with low sampling and switching frequency while others require higher frequencies. All methods have good dynamic behavior, which is acceptable for all main practical applications.

The resonance of the input filter is a key issue in the operation of MCs. An important observation, not previously highlighted,

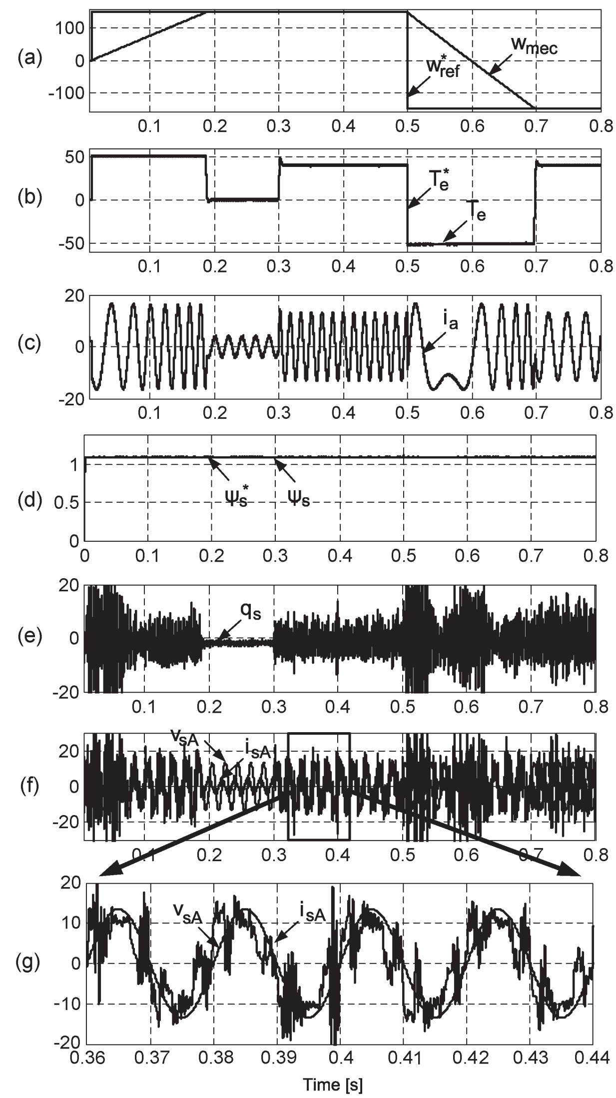

Fig. 12. Predictive control torque without power factor correction $\lambda_q = 0$. (a) Speed (in radians per second). (b) Electrical torque (in newton meters). (c) Output current (in amperes). (d) Stator flux (in webers). (e) Reactive power (in kvar). (f) Input current (in amperes) and input voltage (V/30). (g) Zoom of input current i_{sA} and input voltage v_{sA}.

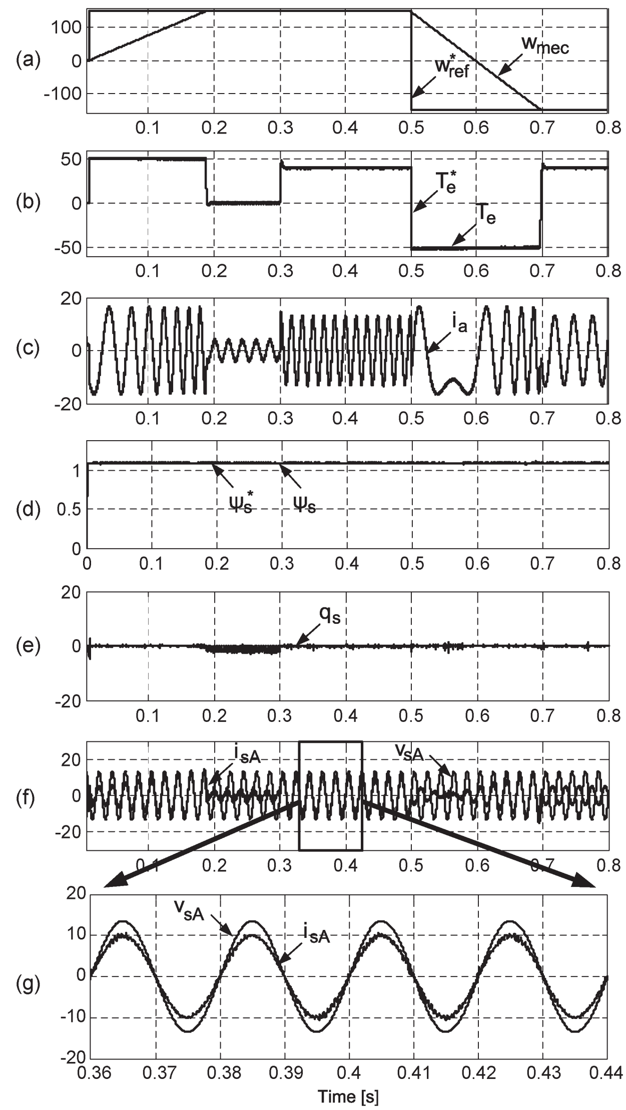

Fig. 13. Predictive control torque with power factor correction $\lambda_q = 1$. (a) Speed (in radians per second). (b) Electrical torque (in newton meters). (c) Output current (in amperes). (d) Stator flux (in webers). (e) Reactive power (in kvar). (f) Input current (in amperes) and input voltage (V/30). (g) Zoom of input current i_{sA} and input voltage v_{sA}.

is that a control or modulation method has a very significant influence on the behavior of the input filter [74], [86]. In effect, methods working with fixed switching frequency, like Venturini, Roy, and SVM, have a reduced resonance in the input filter. Carrier-based methods that do not take care of the quality of the input current originate strong resonances in the input filter. This behavior can be drastically improved taking into consideration the input current. DTC has very strong resonances in the input filter, while predictive techniques have mixed results. The introduction of the control of the reactive power in the quality function introduces an important reduction of the resonance in predictive methods [10], [67], [73], [76], [78], [80], [84].

Other techniques that have been applied to MCs are fuzzy control [87], [88], neural networks [89], [90], genetic algorithms [91], [92], etc. In addition, new topologies of ac–ac converters such as sparse and z-source converters for specific applications have been proposed, as well as a study from the manufacturer's perspective, as reported in [93]–[100].

IX. Comments and Conclusion

The area of MCs has shown continuous development in recent years in terms of new topologies, new control methods, and applications. This paper has presented a number of control methods that are highly investigated today, which, in principle, exhibit good performance [17], [27], [54]. These methods have different theoretical principles and different degrees of complexity.

With the results reported in this paper, predictive control appears as the most promising alternative due to its simplicity and flexibility to include additional aspects in the control. However, with the results reported to date in the literature, it is not possible to establish which method is the best. The authors consider that deeper research must be done in the future to clarify the advantages of each method or to select the best alternative. This comparison must include more advanced

TABLE II
COMPARISON BETWEEN CONTROL AND MODULATION METHODS FOR MCs

	Venturini	**Scalar**	**Carrier Based PWM**	**Space Vector Modulation**	**Direct Torque Control**	**Predictive Current Control**	**Predictive Torque Control**
Complexity	low	low	very low	very high	high	low	low
Sampling frequency	very low	very low	low	low	very high	high	high
Switching frequency	very low	very low	low	low	high	high	high
Dynamic response	good	good	good	good	fast	very fast	very fast
Resonance input filter	low	low	medium	low	very high	from very high to low	from very high to low

aspects such as detailed evaluation of losses, system integration, electromagnetic compatibility, etc.

REFERENCES

[1] E. Yamamoto, T. Kume, H. Hara, T. Uchino, J. Kang, and H. Krug, "Development of matrix converter and its applications in industry," in *Proc. 35th IEEE IECON*, Porto, Portugal, 2009, pp. 4–12.

[2] M. Venturini, "A new sine wave in sine wave out, conversion technique which eliminates reactive elements," in *Proc. Powercon 7*, 1980, pp. E3/1–E3/15.

[3] J. Rodriguez, E. Silva, F. Blaabjerg, P. Wheeler, J. Clare, and J. Pontt, "Matrix converter controlled with the direct transfer function approach: Analysis, modelling and simulation," *Int. J. Electron.*, vol. 92, no. 2, pp. 63–85, Feb. 2005.

[4] L. Zhang, C. Watthanasarn, and W. Shepherd, "Control of AC–AC matrix converters for unbalanced and/or distorted supply voltage," in *Proc. 32nd Annu. IEEE Power Electron. Spec. Conf.*, 2001, vol. 2, pp. 1108–1113.

[5] G. Roy and G.-E. April, "Cycloconverter operation under a new scalar control algorithm," in *Proc. 20th Annu. IEEE Power Electron. Spec. Conf.*, Jun. 1989, vol. 1, pp. 368–375.

[6] J. Rodriguez, "High performance dc motor drive using a PWM rectifier with power transistors," *Proc. Inst. Elect. Eng. B—Elect. Power Appl.*, vol. 134, no. 1, p. 9, Jan. 1987.

[7] L. Huber and D. Borojevic, "Space vector modulated three-phase to three-phase matrix converter with input power factor correction," *IEEE Trans. Ind. Appl.*, vol. 31, no. 6, pp. 1234–1246, Nov. 1995.

[8] F. Blaabjerg, D. Casadei, C. Klumpner, and M. Matteini, "Comparison of two current modulation strategies for matrix converters under unbalanced input voltage conditions," *IEEE Trans. Ind. Electron.*, vol. 49, no. 2, pp. 289–296, Apr. 2002.

[9] I. Takahashi and T. Noguchi, "A new quick response and high efficiency control strategy for an induction motor," *IEEE Trans. Ind. Electron.*, vol. IE-22, no. 5, pp. 820–827, Sep. 1986.

[10] S. Muller, U. Ammann, and S. Rees, "New time-discrete modulation scheme for matrix converters," *IEEE Trans. Ind. Electron.*, vol. 52, no. 6, pp. 1607–1615, Dec. 2005.

[11] M. Rivera, R. Vargas, J. Espinoza, and J. Rodriguez, "Behavior of the predictive DTC based matrix converter under unbalanced AC-supply," in *Proc. IEEE Power Electron. Spec. Conf.*, Sep. 2007, pp. 202–207.

[12] P. Wheeler, J. Rodriguez, J. Clare, L. Empringham, and A. Weinstein, "Matrix converters: A technology review," *IEEE Trans. Ind. Electron.*, vol. 49, no. 2, pp. 276–288, Apr. 2002.

[13] S. Ferreira Pinto and J. Fernando Silva, "Input filter design for sliding mode controlled matrix converters," in *Proc. 32nd Annu. IEEE Power Electron. Spec. Conf.*, 2001, vol. 2, pp. 648–653.

[14] M. Hamouda, F. Fnaiech, and K. Al-Haddad, "Input filter design for SVM dual-bridge matrix converters," in *Proc. IEEE Int. Symp. Ind. Electron.*, Jul. 2006, vol. 2, pp. 797–802.

[15] H. She, H. Lin, X. Wang, and L. Yue, "Damped input filter design of matrix converter," in *Proc. Int. Conf. PEDS*, Nov. 2009, pp. 672–677.

[16] S. Bernet, S. Ponnaluri, and R. Teichmann, "Design and loss comparison of matrix converters, and voltage-source converters for modern AC drives," *IEEE Trans. Ind. Electron.*, vol. 49, no. 2, pp. 304–314, Apr. 2002.

[17] J. Rzasa, "Capacitor clamped multilevel matrix converter controlled with Venturini method," in *Proc. 13th EPE PEMC*, Sep. 2008, pp. 357–364.

[18] Y. Mei and L. Huang, "Improved switching function modulation strategy for three-phase to single-phase matrix converter," in *Proc. IEEE IPEMC*, May 2009, pp. 1734–1737.

[19] S. Lopez Arevalo, P. Zanchetta, P. Wheeler, A. Trentin, and L. Empringham, "Control and implementation of a matrix-converter-based AC-ground power-supply unit for aircraft servicing," *IEEE Trans. Ind. Electron.*, vol. 57, no. 6, pp. 2076–2084, Jun. 2010.

[20] J. Itoh, I. Sato, A. Odaka, H. Ohguchi, H. Kodatchi, and N. Eguchi, "A novel approach to practical matrix converter motor drive system with reverse blocking IGBT," in *Proc. 35th Annu. IEEE Power Electron. Spec. Conf.*, Jun. 2004, vol. 3, pp. 2380–2385.

[21] K. Mohapatra, P. Jose, A. Drolia, G. Aggarwal, and S. Thuta, "A novel carrier-based PWM scheme for matrix converters that is easy to implement," in *Proc. 36th IEEE Power Electron. Spec. Conf.*, Jun. 2005, pp. 2410–2414.

[22] Z. Idris, M. Hamzah, and A. Omar, "Implementation of single-phase matrix converter as a direct AC–AC converter synthesized using sinusoidal pulse width modulation with passive load condition," in *Proc. Int. Conf. PEDS*, Nov. 2005, vol. 2, pp. 1536–1541.

[23] Y.-D. Yoon and S.-K. Sul, "Carrier-based modulation technique for matrix converter," *IEEE Trans. Power Electron.*, vol. 21, no. 6, pp. 1691–1703, Nov. 2006.

[24] T. Satish, K. Mohapatra, and N. Mohan, "Steady state over-modulation of matrix converter using simplified carrier based control," in *Proc. 33rd IEEE IECON*, Nov. 2007, pp. 1817–1822.

[25] P. Loh, R. Rong, F. Blaabjerg, L. Shan, and P. Wang, "Carrier-based modulation schemes for various three-level matrix converters," in *Proc. IEEE Power Electron. Spec. Conf.*, Jun. 2008, pp. 1720–1726.

[26] S. Thuta, K. Mohapatra, and N. Mohan, "Matrix converter over-modulation using carrier-based control: Maximizing the voltage transfer ratio," in *Proc. IEEE Power Electron. Spec. Conf.*, Jun. 2008, pp. 1727–1733.

[27] Y. Miura, S. Horie, S. Kokubo, T. Amano, T. Ise, T. Momose, and Y. Sato, "Application of three-phase to single-phase matrix converter to gas engine cogeneration system," in *Proc. IEEE ECCE*, Sep. 2009, pp. 3290–3297.

[28] P. C. Loh, R. Rong, F. Blaabjerg, and P. Wang, "Digital carrier modulation and sampling issues of matrix converters," *IEEE Trans. Power Electron.*, vol. 24, no. 7, pp. 1690–1700, Jul. 2009.

[29] T. Sanada, S. Ogasawara, and M. Takemoto, "Experimental evaluation of a new PWM control scheme for matrix converters," in *Proc. IPEC*, Jun. 2010, pp. 2366–2371.

[30] P. Kiatsookkanatorn and S. Sangwongwanich, "A unified PWM strategy for matrix converters and its dipolar PWM realization," in *Proc. IPEC*, Jun. 2010, pp. 3072–3079.

[31] T. Yamashita and T. Takeshita, "PWM strategy of single-phase to three-phase matrix converters for reducing a number of commutations," in *Proc. IPEC*, Jun. 2010, pp. 3057–3064.

[32] J. Itoh and K. Maki, "Single-pulse operation for a matrix converter synchronized with the output frequency," in *Proc. IPEC*, Jun. 2010, pp. 2781–2788.

[33] S. Ishii, H. Hara, T. Higuchi, T. Kawachi, K. Yamanaka, N. Koga, T. Kume, and J. Kang, "Bidirectional DC–AC conversion topology using matrix converter technique," in *Proc. IPEC*, Jun. 2010, pp. 2768–2773.

[34] P. Potamianos, E. Mitronikas, and A. Safacas, "A modified carrier-based modulation method for three-phase matrix converters," in *Proc. 13th EPE*, Sep. 2009, pp. 1–9.

[35] Y.-D. Yoon and S.-K. Sul, "Carrier-based modulation method for matrix converter with input power factor control and under unbalanced input voltage conditions," in *Proc. 22nd Annu. IEEE APEC*, Mar. 2007, pp. 310–314.

[36] O. Simon, J. Mahlein, M. Muenzer, and M. Bruckmarm, "Modern solutions for industrial matrix-converter applications," *IEEE Trans. Ind. Electron.*, vol. 49, no. 2, pp. 401–406, Apr. 2002.

[37] D. Casadei, G. Serra, A. Tani, and L. Zarri, "Matrix converter modulation strategies: A new general approach based on space-vector representation of the switch state," *IEEE Trans. Ind. Electron.*, vol. 49, no. 2, pp. 370–381, Apr. 2002.

[38] L. Helle, K. Larsen, A. Jorgensen, S. Munk-Nielsen, and F. Blaabjerg, "Evaluation of modulation schemes for three-phase to three-phase matrix converters," *IEEE Trans. Ind. Electron.*, vol. 51, no. 1, pp. 158–171, Feb. 2004.

[39] D. Casadei, G. Serra, A. Tani, and L. Zarri, "A novel modulation strategy for matrix converters with reduced switching frequency based on output current sensing," in *Proc. 35th Annu. IEEE Power Electron. Spec. Conf.*, Jun. 2004, vol. 3, pp. 2373–2379.

[40] S. Pinto and J. Silva, "Direct control method for matrix converters with input power factor regulation," in *Proc. 35th Annu. IEEE Power Electron. Spec. Conf.*, Jun. 2004, vol. 3, pp. 2366–2372.

[41] M. Jussila, M. Salo, and H. Tuusa, "Induction motor drive fed by a vector modulated indirect matrix converter," in *Proc. 35th Annu. IEEE Power Electron. Spec. Conf.*, 2004, vol. 4, pp. 2862–2868.

[42] L. Wang, D. Zhou, K. Sun, and L. Huang, "A novel method to enhance the voltage transfer ratio of matrix converter," in *Proc. IEEE TENCON*, Nov. 2004, vol. 4, pp. 81–84.

[43] K.-B. Lee and F. Blaabjerg, "Reduced-order extended Luenberger observer based sensorless vector control driven by matrix converter with nonlinearity compensation," *IEEE Trans. Ind. Electron.*, vol. 53, no. 1, pp. 66–75, Feb. 2006.

[44] M. Jussila and H. Tuusa, "Space-vector modulated indirect matrix converter under distorted supply voltage—Effect on load current," in *Proc. IEEE 36th Power Electron. Spec. Conf.*, Jun. 2005, pp. 2396–2402.

[45] F. Gao and M. Iravani, "Dynamic model of a space vector modulated matrix converter," *IEEE Trans. Power Del.*, vol. 22, no. 3, pp. 1696–1705, Jul. 2007.

[46] M. Jussila and H. Tuusa, "Comparison of simple control strategies of space-vector modulated indirect matrix converter under distorted supply voltage," *IEEE Trans. Power Electron.*, vol. 22, no. 1, pp. 139–148, Jan. 2007.

[47] S. Kwak, T. Kim, and O. Vodyakho, "Space vector control methods for two-leg and three-leg based AC to AC converters for two-phase drive systems," in *Proc. 34th IEEE IECON*, Nov. 2008, pp. 959–964.

[48] H.-H. Lee, H. Nguyen, and T.-W. Chun, "New direct-SVM method for matrix converter with main input power factor compensation," in *Proc. 34th IEEE IECON*, Nov. 2008, pp. 1281–1286.

[49] D. Casadei, G. Serra, A. Tani, and L. Zarri, "Optimal use of zero vectors for minimizing the output current distortion in matrix converters," *IEEE Trans. Ind. Electron.*, vol. 56, no. 2, pp. 326–336, Feb. 2009.

[50] H. She, H. Lin, X. Wang, and S. Xiong, "Space vector modulated matrix converter under abnormal input voltage conditions," in *Proc. 6th IEEE IPEMC*, May 2009, pp. 1723–1727.

[51] F. Bradaschia, E. Ibarra, J. Andreu, I. Kortabarria, E. Ormaetxea, and M. Cavalcanti, "Matrix converter: Improvement of the space vector modulation via a new double-sided generalized scalar PWM," in *Proc. 35th IEEE IECON*, Nov. 2009, pp. 4511–4516.

[52] H. Nguyen, H.-H. Lee, and T.-W. Chun, "An investigation on direct space vector modulation methods for matrix converter," in *Proc. 35th IEEE IECON*, Nov. 2009, pp. 4493–4498.

[53] E. Ibarra, J. Andreu, I. Kortabarria, E. Ormaetxea, and E. Robles, "A fault tolerant space vector modulation strategy for matrix converters," in *Proc. 35th IEEE IECON*, Nov. 2009, pp. 4463–4468.

[54] R. Cardenas-Dobson, R. Pena, P. Wheeler, and J. Clare, "Experimental validation of a space vector modulation algorithm for four-leg matrix converters," *IEEE Trans. Ind. Electron.*, vol. 58, no. 4, pp. 1282–1293, Apr. 2011.

[55] M. Nguyen, H. Lee, and T. Chun, "Input power factor compensation algorithms using a new direct-SVM method for matrix converter," *IEEE Trans. Ind. Electron.*, vol. 58, no. 1, pp. 232–243, Jan. 2011.

[56] M. Y. Lee, P. Wheeler, and C. Klumpner, "Space-vector modulated multilevel matrix converter," *IEEE Trans. Ind. Electron.*, vol. 57, no. 10, pp. 3385–3394, Oct. 2010.

[57] E. Ormaetxea, J. Andreu, I. Kortabarria, U. Bidarte, I. Martinez de Alegria, E. Ibarra, and E. Olaguenaga, "Matrix converter protection and computational capabilities based on a system on chip design with an FPGA," *IEEE Trans. Power Electron.*, vol. 26, no. 1, pp. 272–287, Jan. 2011.

[58] M. Kazmierkowski, R. Krishnan, and F. Blaabjerg, *Control in Power Electronics*. New York: Academic, 2002.

[59] D. Casadei, G. Serra, and A. Tani, "The use of matrix converters in direct torque control of induction machines," *IEEE Trans. Ind. Electron.*, vol. 48, no. 6, pp. 1057–1064, Dec. 2001.

[60] C. Ortega, A. Arias, C. Caruana, J. Balcells, and G. Asher, "Improved waveform quality in the direct torque control of matrix-converter-fed PMSM drives," *IEEE Trans. Ind. Electron.*, vol. 57, no. 6, pp. 2101–2110, Jun. 2010.

[61] D. Xiao and F. Rahman, "A modified DTC for matrix converter drives using two switching configurations," in *Proc. 13th EPE*, Sep. 2009, pp. 1–10.

[62] K.-B. Lee and F. Blaabjerg, "Sensorless DTC-SVM for induction motor driven by a matrix converter using a parameter estimation strategy," *IEEE Trans. Ind. Electron.*, vol. 55, no. 2, pp. 512–521, Feb. 2008.

[63] J.-X. Wang and J. guo Jiang, "Variable-structure direct torque control for induction motor driven by a matrix converter with overmodulation strategy," in *Proc. 6th IEEE IPEMC*, May 2009, pp. 580–584.

[64] D. Xiao and F. Rahman, "An improved DTC for matrix converter drives using multi-mode ISVM and unity input power factor correction," in *Proc. 13th EPE*, Sep. 2009, pp. 1–10.

[65] S. Kouro, P. Cortes, R. Vargas, U. Ammann, and J. Rodriguez, "Model predictive control, a simple and powerful method to control power converters," *IEEE Trans. Ind. Electron.*, vol. 56, no. 6, pp. 1826–1838, Jun. 2009.

[66] M. Rivera, R. Vargas, J. Espinoza, J. Rodriguez, P. Wheeler, and C. Silva, "Current control in matrix converters connected to polluted AC voltage supplies," in *Proc. IEEE Power Electron. Spec. Conf.*, Jun. 2008, pp. 412–417.

[67] R. Vargas, J. Rodriguez, U. Ammann, and P. Wheeler, "Predictive current control of an induction machine fed by a matrix converter with reactive power control," *IEEE Trans. Ind. Electron.*, vol. 55, no. 12, pp. 4362–4371, Dec. 2008.

[68] R. Vargas, U. Ammann, J. Rodriguez, and J. Pontt, "Predictive strategy to control common-mode voltage in loads fed by matrix converters," *IEEE Trans. Ind. Electron.*, vol. 55, no. 12, pp. 4372–4380, Dec. 2008.

[69] R. Vargas, U. Ammann, and J. Rodriguez, "Predictive approach to increase efficiency and reduce switching losses on matrix converters," *IEEE Trans. Power Electron.*, vol. 24, no. 4, pp. 894–902, Apr. 2009.

[70] F. Morel, J.-M. Retif, X. Lin-Shi, B. Allard, and P. Bevilacqua, "A predictive control for a matrix converter-fed permanent magnet synchronous machine," in *Proc. IEEE Power Electron. Spec. Conf.*, Jun. 2008, pp. 15–21.

[71] P. Gamboa, J. Silva, S. Pinto, and E. Margato, "Predictive optimal matrix converter control for a dynamic voltage restorer with flywheel energy storage," in *Proc. 35th IEEE IECON*, Nov. 2009, pp. 759–764.

[72] F. Barrero, M. Arahal, R. Gregor, S. Toral, and M. Duran, "One-step modulation predictive current control method for the asymmetrical dual

three-phase induction machine," *IEEE Trans. Ind. Electron.*, vol. 56, no. 6, pp. 1974–1983, Jun. 2009.

[73] P. Correa, J. Rodriguez, M. Rivera, J. Espinoza, and J. Kolar, "Predictive control of an indirect matrix converter," in *IEEE Trans. Ind. Electron.*, Jun. 2009, vol. 56, no. 6, pp. 1847–1853.

[74] M. Rivera, P. Correa, J. Rodriguez, I. Lizama, and J. Espinoza, "Predictive control of the indirect matrix converter with active damping," in *Proc. 6th IEEE IPEMC*, May 2009, pp. 1738–1744.

[75] Y. Li, N.-S. Choi, H. Cha, and F. Peng, "Carrier-based predictive current controlled pulse width modulation for matrix converters," in *Proc. 6th IEEE IPEMC*, May 2009, pp. 1009–1014.

[76] J. Rodriguez, J. Kolar, J. Espinoza, M. Rivera, and C. Rojas, "Predictive current control with reactive power minimization in an indirect matrix converter," in *Proc. IEEE ICIT*, Mar. 2010, pp. 1839–1844.

[77] R. Vargas, J. Rodriguez, C. Rojas, and P. Wheeler, "Predictive current control applied to a matrix converter: An assessment with the direct transfer function approach," in *Proc. IEEE ICIT*, Mar. 2010, pp. 1832–1838.

[78] J. Rodriguez, J. Espinoza, M. Rivera, F. Villarroel, and C. Rojas, "Predictive control of source and load currents in a direct matrix converter," in *Proc. IEEE ICIT*, Mar. 2010, pp. 1826–1831.

[79] J. Rodriguez, J. Pontt, R. Vargas, P. Lezana, U. Ammann, P. Wheeler, and F. Garcia, "Predictive direct torque control of an induction motor fed by a matrix converter," in *Proc. Eur. Conf. Power Electron. Appl.*, Sep. 2007, pp. 1–10.

[80] R. Vargas, M. Rivera, J. Rodriguez, J. Espinoza, and P. Wheeler, "Predictive torque control with input pf correction applied to an induction machine fed by a matrix converter," in *Proc. IEEE Power Electron. Spec. Conf.*, Jun. 2008, pp. 9–14.

[81] C. Ortega, A. Arias, and J. Espina, "Predictive vector selector for direct torque control of matrix converter fed induction motors," in *Proc. 35th IEEE IECON*, Nov. 2009, pp. 1240–1245.

[82] T. Geyer, G. Papafotiou, and M. Morari, "Model predictive direct torque control—Part I: Concept, algorithm, and analysis," *IEEE Trans. Ind. Electron.*, vol. 56, no. 6, pp. 1894–1905, Jun. 2009.

[83] G. Papafotiou, J. Kley, K. Papadopoulos, P. Bohren, and M. Morari, "Model predictive direct torque control—Part II: Implementation and experimental evaluation," *IEEE Trans. Ind. Electron.*, vol. 56, no. 6, pp. 1906–1915, Jun. 2009.

[84] R. Vargas, U. Ammann, B. Hudoffsky, J. Rodriguez, and P. Wheeler, "Predictive torque control of an induction machine fed by a matrix converter with reactive input power control," *IEEE Trans. Power Electron.*, vol. 25, no. 6, pp. 1426–1438, Jun. 2010.

[85] J. Rodriguez, J. Kolar, J. Espinoza, M. Rivera, and C. Rojas, "Predictive torque and flux control of an induction machine fed by an indirect matrix converter," in *Proc. IEEE ICIT*, Mar. 2010, pp. 1857–1863.

[86] J. Itoh, K. Koiwa, and K. Kato, "Input current stabilization control of a matrix converter with boost-up functionality," in *Proc. IPEC*, Jun. 2010, pp. 2708–2714.

[87] H. Karaca, R. Akkaya, and H. Dogan, "A novel compensation method based on fuzzy logic control for matrix converter under distorted input voltage conditions," in *Proc. 18th Int. Conf. Elect. Mach.*, Sep. 2008, pp. 1–5.

[88] K. Park, E.-S. Lee, and K.-B. Lee, "A Z-source sparse matrix converter with a fuzzy logic controller based compensation method under abnormal input voltage conditions," in *Proc. IEEE ISIE*, Jul. 2010, pp. 614–619.

[89] P. Q. Dzung and L. M. Phuong, "A new artificial neural network—Direct torque control for matrix converter fed three-phase induction motor," in *Proc. Int. Conf. PEDS*, 2005, vol. 1, pp. 78–83.

[90] H. H. Lee, P. Q. Dzung, L. M. Phuong, and L. D. Khoa, "A new artificial neural network controller for direct control method for matrix converters," in *Proc. Int. Conf. PEDS*, Nov. 2009, pp. 434–439.

[91] P. Zanchetta, M. Sumner, J. Clare, and P. Wheeler, "Control of matrix converters for AC power supplies using genetic algorithms," in *Proc. IEEE Ind. Electron.*, May 2004, vol. 2, pp. 1429–1433.

[92] P. Zanchetta, J. Clare, P. Wheeler, M. Bland, L. Empringham, and D. Katsis, "Control design of a three-phase matrix converter mobile ac power supply using genetic algorithms," in *Proc. 36th IEEE Power Electron. Spec. Conf.*, Jun. 2005, pp. 2370–2375.

[93] J. Kolar, T. Friedli, F. Krismer, and S. Round, "The essence of three-phase AC/AC converter systems," in *Proc. 13th EPE-PEMC*, Sep. 2008, pp. 27–42.

[94] X. Liu, P. C. Loh, F. Z. Peng, and P. Wang, "Optimal modulation of indirect Z-source matrix converter," in *Proc. IPEC*, Jun. 2010, pp. 3049–3056.

[95] D. Zhou, K. Phillips, G. Skibinski, J. McCarty, M. Loth, B. Buchholz, D. Braun, and R. Lukaszweski, "Evaluation of AC–AC matrix converter, a manufacturer's perspective," in *Conf. Rec. 37th IEEE IAS Annu. Meeting*, 2002, pp. 1558–1563.

[96] C. Klumpner, P. Nielsen, I. Boldea, and F. Blaabjerg, "A new matrix converter motor (MCM) for industry applications," *IEEE Trans. Ind. Electron.*, vol. 49, no. 2, pp. 325–335, Apr. 2002.

[97] K. Yamada, T. Higuchi, E. Yamamoto, H. Hara, T. Sawa, M. Swamy, and T. Kume, "Filtering techniques for matrix converters to achieve environmentally harmonious drives," in *Proc. Eur. Conf. Power Electron. Appl.*, 2005, p. 10.

[98] P. Wheeler, J. Clare, M. Apap, L. Empringham, K. Bradley, S. Pickering, and D. Lampard, "A fully integrated 30 kW motor drive using matrix converter technology," in *Proc. Eur. Conf. Power Electron. Appl.*, 2005, p. 9.

[99] T. Hatase, T. Abe, T. Higuchi, and H. Hara, "Improvement of output voltage waveform for ARCP matrix converter," in *Proc. 13th EPE*, Sep. 2009, pp. 1–8.

[100] R. Bucknall and K. Ciaramella, "On the conceptual design and performance of a matrix converter for marine electric propulsion," *IEEE Trans. Power Electron.*, vol. 25, no. 6, pp. 1497–1508, Jun. 2010.

Jose Rodriguez (M'81–SM'94–F'10) received the Engineer degree in electrical engineering from Universidad Técnica Federico Santa María (UTFSM), Valparaíso, Chile, in 1977 and the Dr.-Ing. degree in electrical engineering from the University of Erlangen, Erlangen, Germany, in 1985.

Since 1977, he has been with the Department of Electronics Engineering, UTFSM, where he is currently a Full Professor and a Rector. He has coauthored more than 300 journal and conference papers. His main research interests include multilevel inverters, new converter topologies, control of power converters, and adjustable-speed drives.

Dr. Rodriguez was a recipient of the Best Paper Award from the IEEE TRANSACTIONS ON INDUSTRIAL ELECTRONICS in 2007 and the IEEE INDUSTRIAL ELECTRONICS MAGAZINE in 2008. He is member of the Chilean Academy of Engineering.

Marco Rivera (S'09–M'11) received the B.Sc. degree in electronics engineering and M.Sc. degree in electrical engineering from the Universidad de Concepción, Concepción, Chile, in 2007 and 2008, respectively. He is currently working toward the Ph.D. degree in the Department of Electronics Engineering, Universidad Técnica Federico Santa María, Valparaíso, Chile, with a scholarship from the Chilean research fund Comisión Nacional de Investigación Científica y Tecnológica, where he is currently working on his Ph.D. thesis.

During January and February of 2010, he was a visiting Ph.D. student in the Electrical and Computer Engineering Department, Ryerson University, Toronto, ON, Canada, where he worked on predictive control applied on four-leg inverters. He was also a visiting Ph.D. student in the Departamento de Ingeniería Eléctrica y Computacional, Instituto Tecnológico y de Estudios Superiores de Monterrey, Monterrey, Mexico, where he worked on the experimental aspects of a doubly fed induction generator and indirect matrix converter system. He is currently a part-time Professor of digital signal processors and design of electronics devices with Universidad Técnica Federico Santa María. His research interests include direct and indirect matrix converters, predictive and digital controls for high-power drives, four-leg converters, and development of high-performance control platforms based on field-programmable gate arrays.

Mr. Rivera was awarded a scholarship from the Marie Curie Host Fellowships for Early Stage Research Training in Electrical Energy Conversion and Conditioning Technology at University College Cork, Cork, Ireland.

Johann W. Kolar (M'89–SM'04–F'10) received the M.Sc. and Ph.D. degrees (*summa cum laude/ promotio sub auspiciis praesidentis rei publicae*) from Vienna University of Technology, Vienna, Austria.

Since February 1, 2001, he has been a Professor and the Head of the Power Electronic Systems Laboratory, Swiss Federal Institute of Technology (ETH) Zurich, Zurich, Switzerland. He has proposed numerous novel PWM converter topologies, and modulation and control concepts, e.g., the Vienna Rectifier, the Swiss Rectifier, and the Three-Phase AC–AC Sparse Matrix Converter. He has published over 400 scientific papers in international journals and conference proceedings and has filed more than 80 patents.

Patrick W. Wheeler (M'00) received the Ph.D. degree in electrical engineering from the University of Bristol, Bristol, U.K., in 1993, for his work on matrix converters.

Since 1993, he has been with the School of Electrical and Electronic Engineering, The University of Nottingham, Nottingham, U.K., first as a Research Assistant, then as a Lecturer in power electronic systems with the Power Electronics, Machines, and Control Group in 1996, as a Senior Lecturer in 2002, and as a Professor since 2007. His research interests include variable-speed ac motor drives, particularly different circuit topologies; power converters for power systems; and semiconductor switch use.